Pt Nanoparticle-Dispersed Graphene-Wrapped MWNT Composites As Oxygen Reduction Reaction Electrocatalyst in Proton Exchange Membrane Fuel Cell

ARTICLE *in* ACS APPLIED MATERIALS & INTERFACES · AUGUST 2012

Impact Factor: 6.72 · DOI: 10.1021/am301187h · Source: PubMed

2 AUTHORS:

Jyothirmayee Aravind
Wright State University
25 PUBLICATIONS **449** CITATIONS
SEE PROFILE

Ramaprabhu Sundara
Indian Institute of Technology Madras
57 PUBLICATIONS **1,118** CITATIONS
SEE PROFILE

ACS APPLIED MATERIALS & INTERFACES

Research Article

www.acsami.org

Pt Nanoparticle-Dispersed Graphene-Wrapped MWNT Composites As Oxygen Reduction Reaction Electrocatalyst in Proton Exchange Membrane Fuel Cell

S. S. Jyothirmayee Aravind and Sundara Ramaprabhu*

Alternative Energy and Nanotechnology Laboratory (AENL), Nanofunctional Materials Technology Center (NFMTC), Department of Physics, Indian Institute of Technology Madras, Chennai 600036, India

Supporting Information

ABSTRACT: Chemical and electrical synergies between graphite oxide and multiwalled carbon nanotube (MWNT) for processing graphene wrapped-MWNT hybrids has been realized by chemical vapor deposition without any chemical functionalization. Potential of the hybrid composites have been demonstrated by employing them as electrocatalyst supports in proton exchange membrane fuel cells. The defects present in the polyelectrolyte, which have been wrapped over highly dispersed MWNT, act as anchoring sites for the homogeneous deposition of platinum nanoparticles. Single-cell proton exchange membrane fuel cells show that the power density of the hybrid composite-based fuel cells is higher compared to the pure catalyst-support-based fuel cells, because of enhanced electrochemical reactivity and good surface area of the nanocomposites.

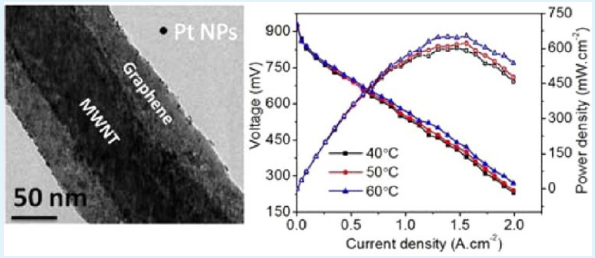

KEYWORDS: *graphene, carbon nanotube, Pt nanoparticles, chemical vapor deposition, fuel cells, power density*

The rapid devastation of nonrenewable energy sources demanded the development of alternative energy conversion devices such as fuel cells with high efficiency and environmental benignity.[1−3] The commercialization of proton exchange membrane fuel cell (PEMFC) is still not achieved because of the high cost of the electrocatalyst, platinum (Pt). In this context, efficient dispersion of Pt nanoparticle over suitable catalyst supports is an eye-catching arena in fuel cell research. The ideal electrode must possess high specific surface area and be decorated with well-dispersed electrocatalyst.[4] This criterion is essential because the catalytic reduction of oxygen (at cathode) and catalytic oxidation (at anode) are both surface processes. Carbon supported electrocatalysts have been found to be effective in reducing the amount of platinum and enhancing the PEMFC performance.[5,6] Carbon black has been employed as catalyst support for quiet long time.[7−10] A commodious support for an electrocatalyst should have high surface area, good electrical properties and high electrochemical stability under PEM fuel cell operating conditions. With high specific surface area, good conductivity, lightweight and high chemical stability, carbon nanotubes (CNT) are one of the most attractive nanomaterials used as an efficient catalyst support in energy systems like hydrogen storage,[11] super-capacitors[12] and fuel cells.[13] To fabricate an efficient catalyst support, one of the most challenging tasks is how to deposit metal catalyst nanoparticles uniformly onto the surface of CNT with strong adherence. Pretreatment of CNT with harsh oxidative acids is often required to generate functional groups on sidewalls as nucleation sites for deposition of well dispersed, adherent Pt clusters.[14] However, the acid treatment produced defects on the CNT surface could lower its conductivity. Hence, alternative methods, which do not involve harsh chemical treatments for the functionalization of CNT, can be promising for electrochemical applications.

Recent discovery of two-dimensional graphene has created an increasing interest in material science community due to its fascinating properties. Graphene exhibits properties almost similar to that of CNT including high aspect ratio, high electrical and mechanical properties, and high surface area, and hence, is expected to be exploited for similar applications fields as that of CNT.[15,16] Graphene has already been explored for fuel cell applications.[17−19] As-synthesized graphene, because of the removal of functional groups over the basal planes of graphite oxide (GO), is highly hydrophobic. Any solution-processing technique demands suitable functionalization of graphene. The process of functionalization of graphene is known to induce restacking of separated graphene sheets and hence limiting its application. It is predicted that CNT can be employed as a space impediment between the graphene sheets to prevent the restacking of graphene (19). In recent years, composite materials of CNT and graphene stimulated wide interest to establish synergistic effects between these two different graphitic nanostructures. Attempts to integrate CNT and graphene have been made in the application fields of transparent conductors and electrode materials for rechargeable

Received: December 5, 2011
Accepted: August 1, 2012
Published: August 1, 2012

lithium ion secondary batteries.[20,21] The combination of one-dimensional CNT and two-dimensional graphene can be exceptionally advantageous when employed as a catalyst support material in fuel cell. 1D−2D combination of CNT-graphene as catalyst support material in PEMFC has been investigated.[19,22] The full-scale implementation of combining CNT and graphene can be obtained by establishing a direct connection between these two materials. Recently, we have reported the synthesis of novel one-dimensional smooth and wrinkled graphene wrapped multi walled carbon nanotube (MWNT) hybrid composites by chemical vapor deposition (CVD) technique.[23] In the present work, the potential of the highly defective and high conducting polyelectrolyte (graphene) wrapped MWNT composites have been demonstrated by employing them as electrocatalyst support in proton exchange membrane fuel cells (PEMFC). Without any harsh chemical functionalization, the composites dispersed well in aqueous solvents and homogeneous dispersion of Pt nanoparticles was achieved by ethylene glycol (EG) reduction method. The enhanced power density of the graphene wrapped MWNT composites based fuel cell over commercial catalyst as well as pure carbon nanomaterials has been reported. Further, the stability analysis of the nanocomposites based PEMFC has been performed and the results are discussed.

Graphite oxide (GO) was prepared by Hummer's method.[24] Hybrid nanocomposites of graphene and MWNT were prepared by thermal CVD using a mixture of $MmNi_3$ alloy hydride catalyst and GO in different weight ratios. Smooth and wrinkled graphene wrapping over MWNT is accomplished by allowing hydrogen at 500 and 240 °C and the respective synthesized samples are labeled as graphene-MWNT-500 (GC-500) and graphene-MWNT-240 (GC-240). Further, different weight ratios of GO and f-MWNT were taken in order to prepare graphene-MWNT with different weight ratios by allowing hydrogen at 500 °C. GC-500 samples prepared by using GO-MWNT in 1:1, 1:2, and 2:1 ratios are designated as GC-500 (1:1), GC-500 (1:2), and GC-500 (2:1) respectively. Multiwalled carbon nanotubes were prepared by chemical vapor deposition of $MmNi_3$ catalyst in CVD.[25] The as-grown sample was purified by air oxidation and acid treatment and then functionalized by treating with conc. HNO_3 for 1 h. This functionalized MWNT is termed as f-MWNT. As a control sample, pure graphene is prepared by hydrogen exfoliation of GO[26] and is functionalized by magnetic stirring in conc. HNO_3 for 1 h (f-HEG). The Pt loading over these carbon nanomaterials has been achieved by EG reduction technique[27] using $H_2PtCl_6.6H_2O$ as Pt precursor. The Pt dispersed carbon nanomaterials together with commercial Pt/carbon with 20 wt % Pt loading (Arora Matthey Limited) has been tested for PEMFC applications.

The formation of the composites has been verified by powder X-ray diffractograms. Figure 1A shows the XRD of GO and purified graphene-wrapped MWNT composites. The introduction of oxygen containing functional groups on GO has resulted in a change in interlayer distance in GO (~0.8 nm) compared to that of graphite (0.34 nm). The formation of the hybrid composites is verified by XRD pattern, as the peak corresponding to GO has been shifted to a higher 2θ value. Graphene-MWNT-240 and graphene-MWNT-500 exhibits intense peaks at nearly 26° with an interlayer d spacing of ~0.34 nm. The broadness of the XRD intensities is an indication of the formation of nanometer-sized crystallites. In Figure 1B, XRD of Pt-dispersed graphene−MWNT composites

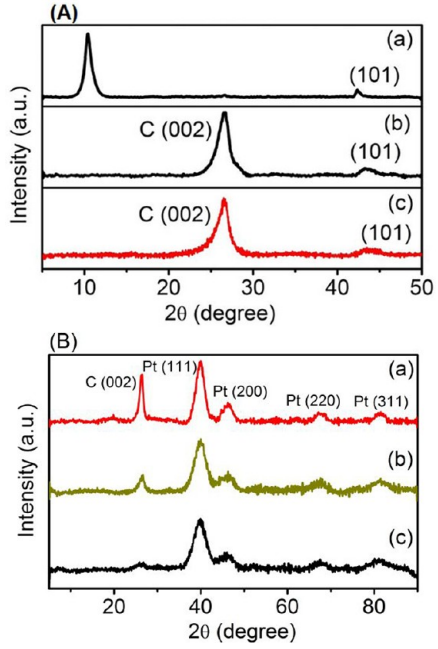

Figure 1. (A) XRD spectra of (a) GO, (b) GC-240, (c) GC-500 (1:1); and (B) XRD spectra of (a) Pt/f-MWNT, (b) Pt/GC-500 (1:1), and (c) Pt/GC-240.

exhibit a peak at ~26° corresponding to reflections from hexagonal graphite. This peak commonly appears in both MWNT and graphene. Besides, the characteristic face centered cubic (fcc) platinum lattice expose diffraction peaks at 39.9° for Pt (111), 46.3° for Pt (200), 67.6° for Pt (220), and 81.4° for Pt (311). This confirms that the platinum precursor has been reduced to platinum by EG reduction technique. The diffraction peak for Pt (220) is used to estimate the platinum crystallite size because there is no interference from other diffraction peaks. The Scherrer equation yields an average crystallite size of Pt (normal to Pt (220)) on GC-500 and GC-240 of 2.4 nm. By assuming that platinum nanoparticles are spherical, Pt surface area is calculated as 66 m^2/g. The particle size of Pt over f-MWNT is calculated as 3.4 nm. XRD of Pt/C, Pt/f-HEG, Pt/GC-500 (1:2) and Pt/GC-500 (2:1) depicted in Figure S1 confirms the decoration of Pt nanoparticles over the carbon nanostructures. The Pt particle sizes calculated from Scherrer formula for Pt/C, Pt/f-HEG, Pt/GC-500 (1:2), and Pt/GC-500 (2:1) are respectively 6.9, 4.2, 4.4, and 3.4 nm.

The hetero structure of the composites can be verified by the morphological analyses. Figure 2 displays the TEM images of the hybrid nanocomposites. Wrinkled and smooth graphene wrapped MWNT obtained under different experimental conditions are clearly visible from these images. The graphene

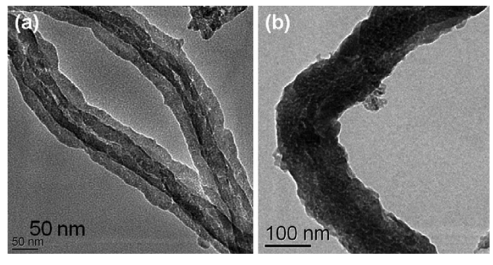

Figure 2. TEM images of (a) GC-500 and (b) GC-240.

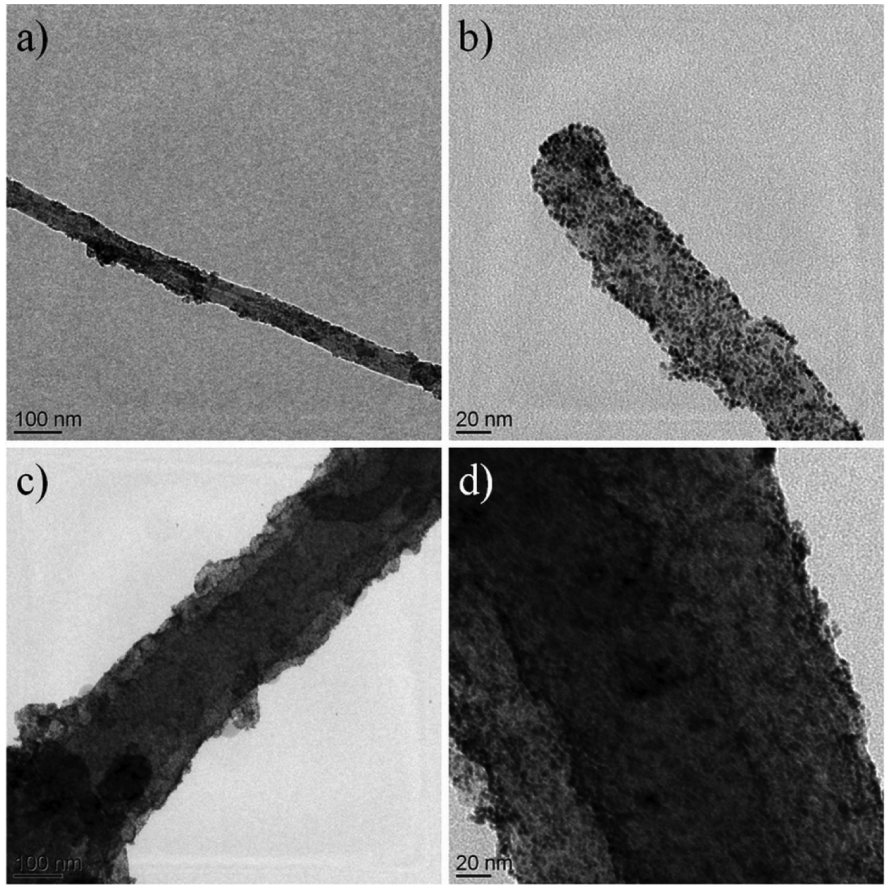

Figure 3. (a) TEM and (b) HRTEM images of Pt/GC-500 and (c) TEM and (d) HRTEM images of Pt/GC-240.

coating is uniform throughout MWNT in both the composites. The diameters of GC-500 and GC-240 are 60−70 nm and 120−140 nm, respectively. The morphology of graphene-MWNT with 1:2 and 2:1 ratios is depicted in Figure S2 in the Supporting Information. It is noted that when the weight ratio of precursors is changed from 1:1, a corresponding change manifested in the composite material. For instance, doubling the amount of GO has resulted in thicker coating of graphene over MWNT in the case of GC-500 (2:1) compared to thin layer coating with GC-500 (1:2). Further, a clear coating of graphene over MWNT is perceptible with GC-500 (2:1) composite; where as the thin coating of graphene over MWNT is preventing the clear contrast between graphene and MWNT. The diameter of GC-500 (1:2) and GC-500 (2:1) is in the range of 90−110 nm and 140−160 nm, respectively.

We found that the anchored Pt nanoparticles distributed uniformly on these hybrid nanocomposites without obvious aggregations (Figure 3). The exceptionally good dispersion of metal nanoparticles on supports is highly advantageous in catalytic as well as sensing activities. The particle size of Pt has been in the range of 2−2.2 nm and 1.8−2 nm for Pt/GC-500 and Pt/GC-240 respectively (Figure 3b, d). TEM image of Pt/C shows coating of Pt over Vulcan carbon (see Figure S3 in the Supporting Information). Even though the coating of Pt over f-HEG is uniform, agglomeration of particles also can be seen. On the other hand, uniform deposition of Pt nanoparticles can be seen in the case of GC-500 (2:1), GC-500 (1:2) and f-MWNT. The particle sizes of Pt over GC-500 (1:2) and GC-500 (2:1) are found to be 4.6−5.3 nm and 3.5−4.3 nm, respectively.

Raman spectrum analysis has been carried out using 532 nm laser excitation (2.33 eV) and is shown in Figure S4 in the Supporting Information. Two major peaks appear in the Raman spectrum of hybrid nanomaterials, i.e., the G band at ∼1567 cm^{-1}, which arises because of first-order Raman scattering of the E_{2g} phonon at the Brillouin zone center of sp^2 carbon atoms[28] and a band at 1356 cm^{-1} known as D mode corresponds to defects present in the material.[29] Raman spectrum of GC-240 exhibits a D band at ∼1337 cm^{-1} and a G peak at ∼1579 cm^{-1} where as the D and G peaks of GC-500 arise at ∼1336 cm^{-1} and ∼1581 cm^{-1}. The intensity ratio of D band to the G band (I_D/I_G) of GC-500 is 1.05 where as that of GC-240 is 1.23. The increase in I_D/I_G of GC-240 is an indication that wrapping of the wrinkled graphene around MWNT induces more defects due to the presence of functional groups. The crystallite size (La) of the composites has been determined using the equation, La = $4.4/(I_D/I_G)$[30] and it is found to be 2.76 and 3.43 nm for GC-240 and GC-500, respectively. The less crystallite size values of the composites can be advantageous for electrochemical applications.

The electrical conductivity of graphene wrapped MWNT composites have been measured and compared (Figure 4) with that of graphene synthesized by thermal exfoliation (*G*) at 1050 °C and MWNT prepared by CVD technique. The electrical conductivity of conducting samples have been measured using linear four probe method whereas two probe technique was used for measuring the conductivity of insulating GO. An enhancement in electronic conjugation of the hybrid nanocomposites has been observed compared with pure MWNT or graphene. These high electrical conductivities of the hybrid

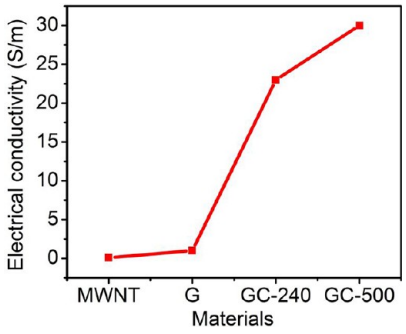

Figure 4. Electrical conductivity of different types of carbon nanomaterials.

nanocomposites find potential applications in the field of fuel cells, super capacitors, polymer nanocomposites etc. BET surface area of the hybrid nanocomposites has been measured via nitrogen gas absorption and the values are 117 m^2/g and 139 m^2/g for graphene-MWNT-240 and graphene-MWNT-500 respectively (see Figure S6 in the Supporting Information). The enhanced specific surface area of the nanocomposites compared to that of pure MWNT (91.9 m^2/g) prepared by CVD, indicates the superiority of graphene coated MWNT over pure MWNT.

The potential usage of the graphene coated MWNT composites in device applications has been evaluated by fabricating PEM fuel cells. The membrane electrode assembly (MEA) was prepared by sandwiching a pretreated Nafion 212 CS membrane between the anode and cathode, which constitutes backing layer, gas diffusion layer and catalyst layer. Catalyst slurry was prepared by treating required amount of catalyst with desired amount of Nafion and deionized water by ultrasonication. To be specific, at the anode side, to get 0.25 mg/cm^2 loading of Pt, 12 mg of Pt/f-MWNT was mixed with 0.3 mL of 5 wt % Nafion, whereas at the cathode side, 25 mg of Pt/GC-500 was mixed with 0.6 mL of 5 wt % Nafion to get 0.5 mg/cm^2 loading. The suspension was coated homogeneously over the gas diffusion layer. Composition of the gas diffusion layer is mixture of Vulcan XC 72 carbon and poly tetra fluoro ethylene. The electrodes were sandwiched with Nafion membrane by hot pressing at 130 °C with a force of 1 ton for 4 min. All MEAs were prepared in a similar route, by coating different electrocatalysts (0.5 mg/cm^2 loading) over the cathode keeping Pt/f-MWNT (0.25 mg/cm^2 loading) as the anode catalyst. The effective electrode area is 11.56 cm^2. It is the area where the gas flow is given (groove area of the serpentine graphite flow channel). The MEAs were tested in a fuel cell test station (Electro Chem Fuel Cell Test Station) by fixing them between two graphite plates, which had a provision for gas flow. The H_2 fuel at anode and the O_2 gas at cathode were allowed through respective humidifiers, controlled by their respective mass flow controllers (with flow rates 100 sccm each). All the MEAs were tested under atmospheric pressure.

Figure 5 shows the polarization curves at three different temperatures for MEAs prepared with Pt/GC-500 (1:1), Pt/GC-240, Pt/C, Pt/f-HEG, Pt/f-MWNT, Pt/GC-500 (1:2) and Pt/GC-500 (2:1) as the cathode catalysts with loading of 0.5 mg/cm^2. Pt/f-MWNT with 0.25 mg/cm^2 loading was employed as anode catalyst in all the MEAs in the present study. The performance of these MEAs was tested using the fuel cell test station. Prior to the polarization studies, the electrodes were activated between open circuit potential and high current densities in order to activate the catalyst for the oxygen reduction reaction. The polarization plots were recorded using a dc load box. The GC-240 based fuel cell exhibits an open circuit voltage of 0.94 V. A maximum power density of 607 mW/cm^2 was obtained at 40 °C. It is observed that the cell performance increases when temperature increases, because the catalyst activity and the diffusion coefficient of reactant and the resultant increase with increasing temperature. At 50 °C, the power density is 647 mW/cm^2 and a maximum power density of 661 mW/cm^2 is attained at 60 °C with Pt/GC-240 based MEA. It is observed that there is not much difference in power density with change in morphology of graphene wrapping around MWNT. Further, the performance studies of Pt nanoparticles dispersed over commercial Vulcan carbon, f-HEG, f-MWNT, GC-500 with graphene and MWNT in 2:1 and 1:2 weight ratios has been evaluated and is shown in Figure 5. The maximum power density obtained at 60 °C with Pt/C is 376 mW/cm^2, whereas Pt/f-HEG and Pt/f-MWNT provide a maximum power density of 112 mW/cm^2 and 449 mW/cm^2, respectively. The lower performance with Pt/f-HEG fuel cell can be due to the aggregation of graphene sheets due to van der Waals interaction during the dispersion of Pt nanoparticles. Pt/GC-500 (1:2) and Pt/GC-500 (2:1) exhibit better performance than pure graphene, MWNT or commercial catalyst and the respective polarization power density values being 468 mW/cm^2 and 532 mW/cm^2 at 60 °C. Hence, from the comparative analysis of pure and hybrid carbon nanomaterials as catalyst support in PEMFC, the following conclusions can be drawn. Graphene-wrapped MWNT in hybrid form exhibits better performance than pure MWNT or graphene or commercial Pt/C. By varying the weight ratio of graphene and MWNT or in other words, by tuning the dispersing thickness of graphene over MWNT, difference in fuel cell performance can be observed. Highest performance is obtained with graphene-MWNT obtained with 1:1 ratio of precursors. This can be due to the synergistic effect arising from graphene and MWNT when same quantity of precursors is employed resulting in higher electrocatalytic activity. Also, it is observed that the Pt particle size is low compared to other GC-500 composites and dispersion is uniform in the case of Pt/GC-500 and Pt/GC-240 composites with 1:1 weight ratio.

The higher catalytic activity demonstrated by Pt/GC nanocomposites can be ascribed to the uniform and small particle size of Pt over the composites and also the high electron transfer rates arising from good electrical conductivity. The better performance with the hybrid nanocomposite-based fuel cells can be attributed to several factors. Graphene can be considered as a two-dimensional polyelectrolyte in terms of both structure and property. MWNTs will be entangled together because of the strong van der Waals interactions. The wrapping of graphene around MWNT resulted in composites with well-separated MWNT. The polyelectrolyte coated, highly dispersed MWNT possess anchoring sites, which helps in the homogeneous deposition of ultra nano platinum particles over the composites, without any harsh chemical functionalization. This is evident from the HRTEM image of Pt dispersed GC composites, where the uniform deposition of Pt nanoparticles over the hybrid composites are clearly visible. In the case of one-dimensional graphene-MWNT composites, at a distance of $\leq$0.35 nm, the number of inter fragment van der Waals contacts between graphene and MWNT can reach a maximum. Such a composite may exhibit an extremely wide range of electronic properties, which in turn can be useful for

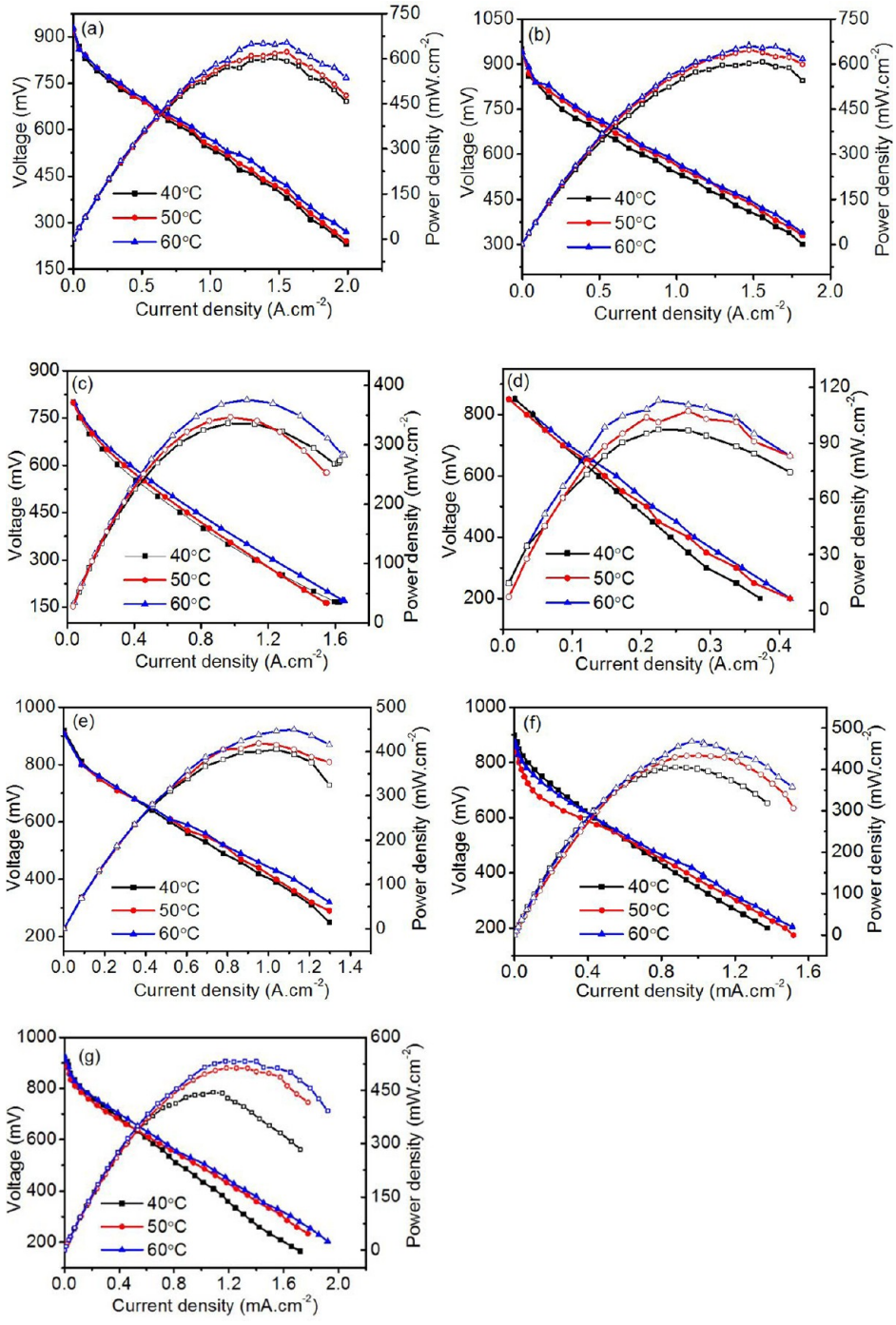

Figure 5. Polarization graphs of fuel cells with (a) Pt/GC-500 (1:1), (b) Pt/GC-240, (c) Pt/C, (d) Pt/f-HEG, (e) Pt/f-MWNT, (f) Pt/GC-500 (1:2), and (g) Pt/GC-500 (2:1) as cathode catalysts and Pt/f-MWNT as anode catalyst.

fuel cell applications.[31] The enhancement in power density with hybrid nanocomposite based MEA can be attributed to the synergistic effect of MWNT and graphene in one-dimensional form. The present novel catalyst support possesses many unique properties such as good conductivity and surface area. Moreover, the EG reduction technique employed for the deposition of Pt nanoparticles results in a more uniform deposition of Pt nanoparticles over the catalyst support. This in turn, enhances the electrocatalyst-carbon support interaction, which leads to the efficient utilization of the catalyst particles in the anode and cathode for fuel cell reaction.

The deterioration of the electrocatalysts is one of the main reasons for the long-term decline in fuel cell performance.[32] Hence, we have investigated the long-term stability of Pt/GC catalysts modified electrodes. The performance of Pt/GC-240 and Pt/GC-500 based fuel cells has been recorded keeping the cells at a constant potential of 0.5 V for a period of 24 h at 60 °C and at atmospheric pressure. Current has been plotted versus time to investigate the stability (Figure 6). The stable current value is an indication of the excellent stability of the present hybrid graphene-wrapped MWNT catalyst supports.

In conclusion, the reported results suggest that the chemical and electrical synergies between two graphene derivatives, GO

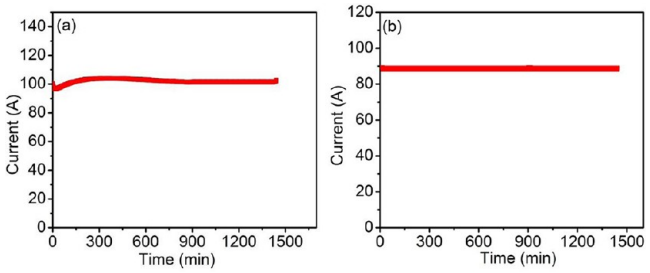

Figure 6. Steady-state performance evaluation of (a) Pt/GC-500 (1:1) and (b) Pt/GC-240 catalysts over a period of 24 h.

and MWNT, can indeed offer an amazingly simple strategy for processing graphene/MWNT monohybrids, in which no chemical functionalization of MWNT is required and no organic solvents, toxic chemicals and surfactants are involved. It also allows convenient integration of the 1D MWNT with 2D graphene to form hierarchically structured carbon monohybrids with enhanced performances. Given that MWNT are essentially rolled graphene sheets and GO is partially oxidized graphene, this work presents an excellent example that fascinating synergetic effects could exist between different graphene derivatives. Dispersing Pt nanoparticles over the nanocomposites with different dispersing thickness of graphene over MWNT and evaluating their PEM fuel cell performance have demonstrated the potential application of the highly defective graphene-MWNT hybrids. The maximum power density accomplished with Pt/GC-240 and Pt/GC-500 based fuel cells are 661 mW/cm^2 and 653 mW/cm^2 respectively. The superior performance of the present carbon hybrid-based fuel cells to commercial Pt/C, pure graphene, and MWNT-based fuel cells can be ascribed to the enhanced electrochemical reactivity and good surface area of the nanocomposites.

■ ASSOCIATED CONTENT

Supporting Information

Experimental section and characterization techniques (XRD, Raman, electrical conductivity and surface area analysis). This material is available free of charge via the Internet at http://pubs.acs.org/.

■ AUTHOR INFORMATION

Corresponding Author

*Email: ramp@iitm.ac.in. Tel: +91-44-22574862. Fax: +91-44-22570509.

Notes

The authors declare no competing financial interest.

■ ACKNOWLEDGMENTS

Financial support from INDO (DST)-UK program and Indian Institute of Technology, Madras is gratefully acknowledged.

■ REFERENCES

(1) Qiao, Y.; Bao, S.-J.; Li, C. M. *Energy. Environ. Sci.* **2010**, *3*, 544–553.
(2) Wang, Y.; Chen, K. S.; Mishler, J.; Cho, S. C.; Adroher, X. C. *Appl. Energy* **2011**, *88*, 981–1007.
(3) Mekhilef, S.; Saidur, R.; Safari, A. *Renewable Sustainable Energy Rev.* **2012**, *16*, 981–989.
(4) Qiao, Y.; Li, C. M. *J. Mater. Chem.* **2011**, *21*, 4027–4036.
(5) Dicks, A. L. *J. Power Sources* **2006**, *156*, 128–141.
(6) Li, W.; Liang, C.; Zhou, W.; Qiu, J.; Zhou; Sun, G.; Xin, Q. *J. Phys. Chem. B* **2003**, *107*, 6292–6299.
(7) Winter, M.; Brodd, R. *J. Chem. Rev.* **2004**, *104*, 4245–4270.
(8) Wei, S.; Wu, D.; Shang, X.; Fu, R. *Energy Fuel* **2009**, *23*, 908–911.
(9) Cai, K.-D.; Yin, G.-P.; Wang, J.-J.; Lu, L.-L. *Energy Fuel* **2009**, *23*, 903–907.
(10) Park, H. I.; Mushtaq, U.; Perello, D.; Lee, I.; Cho, S. K.; Star, A.; Yun, M. *Energy Fuel* **2007**, *21*, 2984–2990.
(11) Leela Mohana Reddy, A.; Ramaprabhu, S. *Int. J. Hydrogen Energy* **2008**, *33*, 1028–1034.
(12) Zhou, C.; Kumar, S.; Doyle, C. D.; Tour, J. M. *Chem. Mater.* **2005**, *17*, 1997–2002.
(13) Lin, Y.; Cui, X.; Yen, C.; Wai, C. M. *J. Phys. Chem. B* **2005**, *109*, 14410–14415.
(14) Yu, R.; Chen, L.; Liu, Q.; Lin, J.; Tan, K.-L.; Ng, S. C.; Chan, H. S. O.; Xu, G.-Q.; Hor, T. S. A. *Chem. Mater.* **1998**, *10*, 718–722.
(15) Du, X.; Skachko, I.; Barker, A.; Andrei, E. Y. *Nat. Nanotechnol.* **2008**, *3*, 491–495.
(16) Lee, C.; Wei, X.; Kysar, J. W.; Hone, J. *Science* **2008**, *321*, 385–388.
(17) Shao, Y.; Zhang, S.; Wang, C.; Nie, Z.; Liu, J.; Wang, Y.; Lin, Y. *J. Power Sources* **2010**, *195*, 4600–4605.
(18) Qu, L.; Liu, Y.; Baek, J.-B.; Dai, L. *ACS Nano* **2010**, *4*, 1321–1326.
(19) Jyothirmayee Aravind, S. S.; Imran Jafri, R.; Rajalakshmi, N.; Ramaprabhu, S. *J. Mater. Chem.* **2011**, *21*, 18199–18204.
(20) Tung, V. C.; Chen, L.-M.; Allen, M. J.; Wassei, J. K.; Nelson, K.; Kaner, R. B.; Yang, Y. *Nano Lett.* **2009**, *9*, 1949–1955.
(21) Yoo, E.; Kim, J.; Hosono, E.; Zhou, H.-s.; Kudo, T.; Honma, I. *Nano Lett.* **2008**, *8*, 2277–2282.
(22) Jafri, R. I.; Arockiadoss, T.; Rajalakshmi, N.; Ramaprabhu, S. *J. Electrochem. Soc.* **2010**, *157*, B874–B879.
(23) Jyothirmayee Aravind, S. S.; Eswaraiah, V.; Ramaprabhu, S. *J. Mater. Chem* **2011**, *21*, 15179–15182.
(24) Hummers, W. S.; Offeman, R. E. *J. Am. Chem. Soc.* **1958**, *80*, 1339.
(25) Reddy, A. L. M.; Shaijumon, M. M.; Ramaprabhu, S. *Nanotechnol.* **2006**, *17*, 5299–5305.
(26) Kaniyoor, A.; Baby, T. T.; Ramaprabhu, S. *J. Mater. Chem.* **2012**, *20*, 8467–8469.
(27) Xing, Y. *J. Phys. Chem. B* **2004**, *108*, 19255–19259.
(28) Dresselhaus, M. S.; Jorio, A.; Hofmann, M.; Dresselhaus, G.; Saito, R. *Nano Lett.* **2010**, *10*, 751–758.
(29) Ferrari, A. C.; Robertson. *J. Phys. Rev. B* **2000**, *61*, 14095–14107.
(30) Subrahmanyam, K. S.; Vivekchand, S. R. C.; Govindaraj, A.; Rao, C. N. R. *J. Mater. Chem.* **2008**, *18*, 1517–1523.
(31) Chernozatonskii, L. A.; Sheka, E. F.; Artyukh, A. A. *JETP Lett.* **2009**, *89*, 352–356.
(32) Xie, J.; Wood, D. L.; More, K. L.; Atanassov, P.; Borup, R. L. *J. Electrochem. Soc.* **2005**, *152*, A1011–A1020.